An ab Initio Molecular Orbital Study of the Mechanism of the Rhodium(I)-Catalyzed Olefin Hydroboration Reaction

Djamaladdin G. Musaev,[†] Alexander M. Mebel,[‡,§] and Keiji Morokuma*[,†,§]

Contribution from the Cherry L. Emerson Center for Scientific Computation and Department of Chemistry, Emory University, Atlanta, Georgia 30322, and Institute Molecular Science, Myodaiji, Okazaki 444, Japan

Received June 14, 1994[⊗]

Abstract: Potential energy surfaces of the rhodium(I)-catalyzed olefin hydroboration reactions, $RhCl(PH_3)_2 + HB(OH)_2 + C_2H_4 \rightarrow RhCl(PH_3)_2 + C_2H_5B(OH)_2$ (**1**) and $RhCl(PH_3)_2 + HBO_2(CH_2)_3 + C_2H_4 \rightarrow RhCl(PH_3)_2 + C_2H_5BO_2(CH_2)_3$ (**2**), have been studied by using ab initio molecular orbital method at the MP2/ECP+DZ level. The following mechanisms have been considered: (**I**) oxidative addition of a B−H bond to the metal center, followed by olefin coordination to the complex in various positions without dissociation of PH_3 group, further followed by insertion of olefin into either M−H or M−B bond and reductive elimination of B−C or B−H bond, respectively and (**II**) coordination of olefin to the metal center, followed by "σ-bond metathesis" involving coordination of borane and simultaneous cleavage of the M−C and B−H bonds with formation of the M−B and H−C or M−H and B−C bonds. For both reactions, the most favorable mechanism is shown to involve oxidative addition of borane to the catalyst and coordination of C_2H_4 to the complex between B and H ligands trans to Cl, followed by insertion of C=C into the Rh−B bond. The reactions are completed by dehydrogenative reductive elimination of C_2H_5BR which is calculated to be the rate determining step and to have the barriers of 22.4 and 20.8 kcal/mol for eqs 1 and 2, respectively. Other competitive mechanisms involve as the rate-controlling step the "σ-bond metathesis" to break B−H and to form M−H and B−C bonds after formation of the $RhCl(PH_3)_2(C_2H_4)$ complex, with the barrier of 23.9 kcal/mol for reaction 1.

I. Introduction

The discovery of transition-metal-catalyzed olefin hydroboration using catecholborane (1,3,2-benzodioxaborole, abbreviated as CB or HBcat where cat = $1,2\text{-}O_2C_6H_4$) and 4,4,6-trimethyl-1,3,2-dioxaborinane (TMDB) has led to the development of applications in organic synthesis and increased the potential applications of boron hydrides in synthetic organic chemistry.[1−4] This process has demonstrated a variety of promising features, including regio-, diastereo-, and chemoselectivity,[1−4] as well as preferential addition to C=C bonds in the presence of more reactive functional groups such as ketones and nitriles.[1] In general, it has been found that (1) the reductive elimination step is the slowest step in the overall transformation; (2) rhodium complexes are most suitable catalysts, among those the Wilkinson catalyst appears to be the most efficient, while the Crabtree's iridium complex,[5] $[Ir(cod)(PCy_3)(py)]PF_6$, is a noteworthy exception in this generalization; (3) boron hydrides bearing oxygen ligands are the most successful reagents, while attempts to catalyze hydroboration of 1-decene with most boron hydrides including bis(benzyloxy)borane, bis(trifluoroacetoxy)borane, tetramethylammonium triacetoxyborohydride, and thexylbornane were unsuccessful; and (4) the rate of the catalyzed hydroboration reaction is very sensitive to the olefin substitution pattern, with terminal alkenes more reactive than highly substituted olefins.[2,3d]

While significant efforts have been focused on the catalyzed hydroboration reactions as a synthetic method, only few investigations have concentrated on the fundamental understanding of elementary steps in the catalytic cycle and the role of transition metal atoms and substrates.[2,3b,e,w,4] The mechanism proposed in early papers[1−3e] for the Wilkinson catalyst involves oxidative addition of a B−H bond to the metal center, followed by olefin coordination to the metal center accompanied with

[†] Emory University.
[‡] Present address: Emory University.
[§] Institute for Molecular Science.
[⊗] Abstract published in *Advance ACS Abstracts,* October 1, 1994.

(1) Manning, D.; Noth, H. *Angew. Chem., Int. Ed. Engl.* **1985**, *24*, 878.
(2) Burgess, K.; Ohlmeyer, M. J. *J. Chem. Rev.* **1991**, *91*, 1179, and references therein.
(3) For leading references see: (a) Evans, D. A.; Fu. G. C.; Hoveyda, A. H. *J. Am. Chem. Soc.* **1988**, *110*, 6917. (b) Evans, D. A.; Fu. G. C. *J. Org. Chem.* **1990**, *55*, 2280. (c) Evans, D. A.; Fu. G. C. *J. Am. Chem. Soc.* **1991**, *113*, 4042. (d) Evans, D. A.; Fu, G. C.; Hoveyda, A. H. *J. Am. Chem. Soc.* **1992**, *114*, 6671. (e) Evans, D. A.; Fu. G. C.; Anderson, B. A. *J. Am. Chem. Soc.* **1992**, *114*, 6679. (f) Burgess, K.; Cassidy, J.; Ohlmeyer, M. J. *J. Org. Chem.* **1991**, *56*, 1020. (g) Burgess, K.; Ohlmeyer, M. J. *J. Org. Chem.* **1991**, *56*, 1027. (h) Burgess, K.; Ohlmeyer, M. *Tetrahedron Lett.* **1989**, *30*, 395. (i) Burgess, K.; Ohlmeyer, M. *Tetrahedron Lett.* **1989**, *30*, 5857. (j) Burgess, K.; Ohlmeyer, M. *Tetrahedron Lett.* **1989**, *30*, 5861. (k) Burgess, K.; van der Donk, W. A.; Jarstfer, M. B.; Ohlmeyer, *J. Am. Chem. Soc.* **1991**, *113*, 6139. (l) Satoh, M.; Nomoto, Y.; Miyaura, N.; Suzuki, A. *Tetrahedron Lett.* **1989**, *30*, 3789. (m) Satoh, M.; Miyaura, N.; Suzuki, A. *Tetrahedron Lett.* **1990**, *31*, 231. (n) Brown, J. M.; Lloyd-Jones, G. C. *Tetrahedron: Asymmetry* **1990**, *1*, 869. (o) Hayashi, T.; Matsumoto, Y.; Ito, Y. *J. Am. Chem. Soc.* **1989**, *111*, 3426. (p) Hayashi, Y.; Matsumoto, Y.; Ito, Y. *Tetrahedron: Asymmetry* **1991**, *2*, 601. (q) Matsumoto, Y.; Hayashi, T. *Tetrahedron Lett.* **1991**, *32*, 3387. (r) Burgess, K.; Ohlmeyer, M. J. *J. Org. Chem.* **1988**, *53*, 5178. (s) Burgess, K.; van der Donk, W. A.; Ohlmeyer, M. J. *Tetrahedron: Asymmetry* **1991**, *2*, 613. (t) Zhang, J.; Lou, B.; Guo, G.; Dai, L. *J. Org. Chem.* **1991**, *56*, 1670. (u) Westcott, S. A.; Slom, H. P.; Marder, T. B.; Baker, R. T. *J. Am. Chem. Soc.* **1992**, *114*, 8863. (v) Westcott, S. A.; Taylor, N. J.; Marder, T. B.; Baker, R. T.; Jones, N. J.; Calabrese, J. C. *J. Chem. Soc., Chem. Commun.* **1991**, 304. (w) Baker, R. T.; Ovenall, D. W.; Calabrese, J. C.; Westcott, S. A.; Taylor, N. J.; Williams, I. D.; Marder, T. B. *J. Am. Chem. Soc.* **1990**, *112*, 9399. (x) Baker, R. T.; Ovenall, D. W.; Harlow, R. L.; Westcott, S. A.; Taylor, N. J.; Marder, T. B. *Organometallics*, **1990**, *9*, 3028. (y) Westcott, S. A.; Blom, H. P.; Marder, T. B.; Baker, R. T.; Calabrese, J. C. *Inorg. Chem.* **1993**, *32*, 2175. (z) Harrison, K. N.; Marks, T. J. *J. Am. Chem. Soc.* **1992**, *114*, 9220. (aa) Burgess, K.; Jaspars, M. *Organometallics*, **1993**, *12*, 497.
(4) (a) Burgess, K.; Donk, W. A.; Kook, A. M. *J. Org. Chem.* **1991**, *56*, 2949. (b) Knorr, J. R.; Merola, J. S. *Organometallics* **1990**, *9*, 3008. (c) Burgess, K.; van der Donk, W. A.; Westcott, S. A.; Marder, T. B.; Baker, R. T.; Calabrese, J. C. *J. Am. Chem. Soc.* **1992**, *114*, 9350.
(5) Crabtree, R. H.; Davis, M. W. *J. Org. Chem.* **1986**, *51*, 2655.

0002-7863/94/1516-10693$04.50/0

Scheme 1. All Possible Mechanisms for Olefin Hydroborations Mediated by $RhCl(PPh_3)_2$

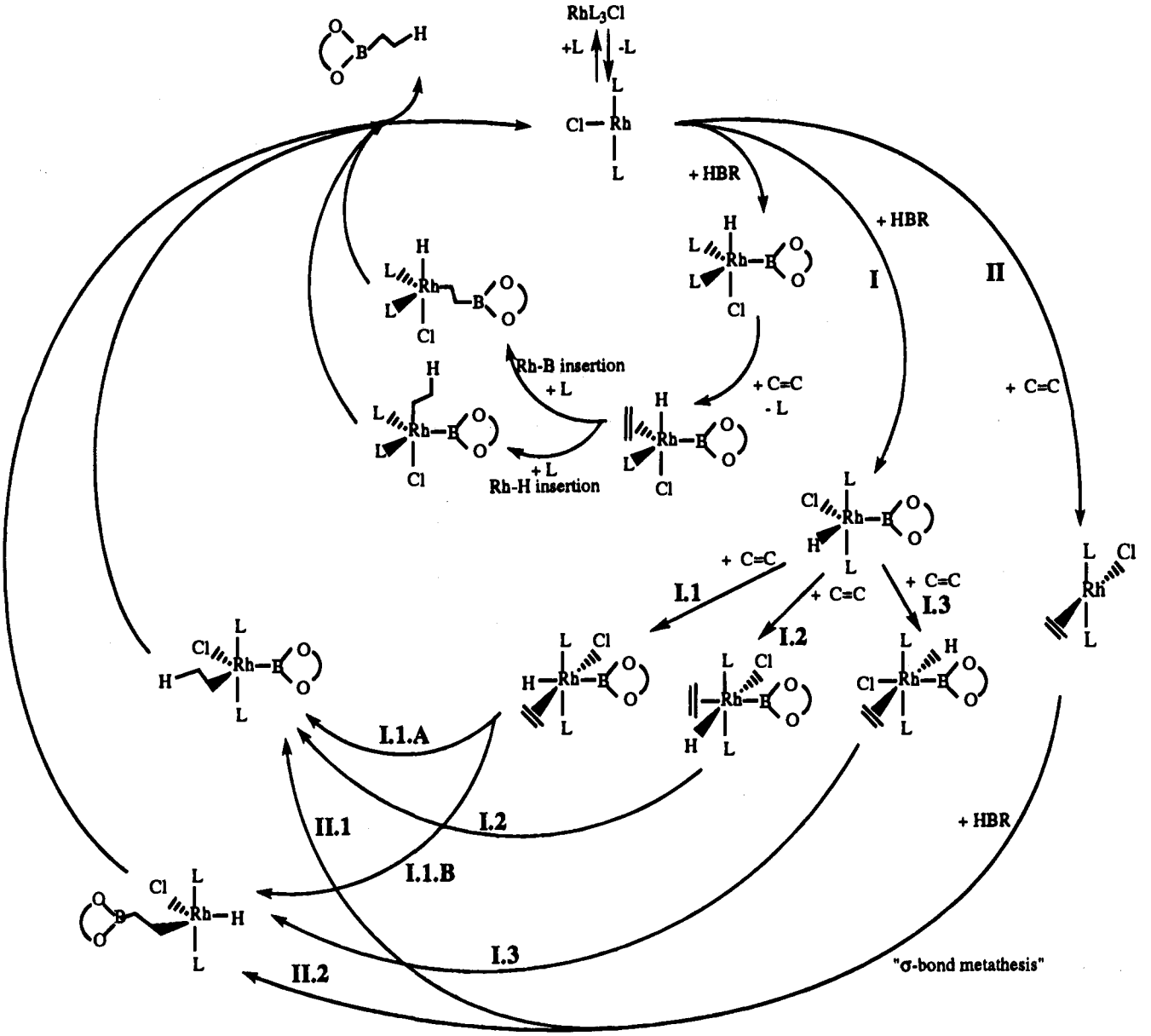

dissociation of one of the two PPh_3, further followed by migratory insertion of olefin into the M−H bond and subsequent reductive elimination of the B−C bond.

Several important questions have been raised concerning this mechanism. First, the phosphine was assumed[1] to dissociate upon olefin coordination and to readd to the complex during one of the next steps. However, Burgess and co-workers later[4c] suggested a mechanism which does not include PPh_3 dissociation. Hence, whether the reaction occurs with phosphine dissociation or not, need to be clarified. Second, Baker and co-workers have recently demonstrated[7] a competitive "dehydrogenative borylation" pathway involving insertion of alkene into the M−B bond and reductive elimination from the resulting borylalkylmetal complex for the reaction of the bis(boryl) complex $(PPh_3)_2RhCl(Bcat)_2$ with 4-vinylanisole. This pathway has also been suggested by recent observations of vinyl boronate esters in several metal-catalyzed olefin hydroborations.[3n,4c,6] It would be interesting to elucidate whether M−B or M−H bond insertion of olefin is more favorable energetically. Third, the latest study of Hartwig and co-workers[8] for the reaction of HBcat addition to $CpRu(PPh_3)_2Me$ complex suggests another possible competitive "σ-bond metathesis" pathway involving coordination of the HBcat to the complex, followed by simultaneous cleavage of the M−CH_3 and B−H bonds with formation of the Ru−H and B−C bonds through a four-center transition state. These proposed mechanisms of the rhodium(I)-catalyzed olefin hydroboration are shown in Scheme 1.

Thus, detailed experimental and theoretical studies are highly desirable on the mechanism of the transition-metal-catalyzed olefin hydroboration reactions as well as on the role of the transition metal center, substrates, and electronic and steric factors in the mechanism. Quantum chemical calculations on the structure and stability of varieties of intermediates and transition states would be extremely useful.

In the present paper, we present the first detailed ab initio molecular orbital study of possible reaction pathways illustrated in Scheme 1, excluding the pathways involving elimination of

(6) Westcott, S. A.; Marder, T. B.; Baker, R. T. *Organometallics* **1993**, *12*, 975.

(7) Baker, R. T.; Calabrese, J. C.; Westcott, S. A.; Nguyen, P.; Marder, T. B. *J. Am. Chem. Soc.* **1993**, *115*, 4367.

(8) Hartwig, J. F.; Bhandari, S.; Rablen, P. R. *J. Am. Chem. Soc.* **1994**, *116*, 1839.

Chart 1. Schematic Representation of d-Orbital Levels for d^8 ML_3 and d^6 ML_5

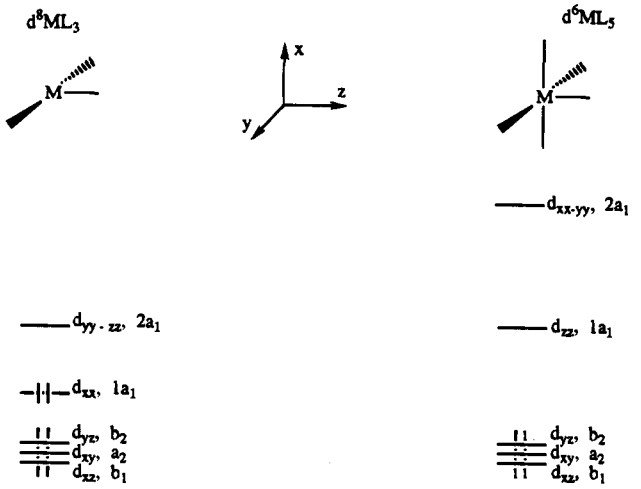

one of the phosphine ligands after olefin coordination. We will study the structure and stability of many intermediates and transition states of the hydroboration reactions of C_2H_4 with the model boranes $HB(OH)_2$ and $HBO_2(CH_2)_3$ involving the model Wilkinson catalyst $RhCl(PH_3)_2$. After the brief section II on the method, we describe results of studies for substrate $HB(OH)_2$ and $HB(CH_2)_3$, in sections III and IV, respectively. Section V is the concluding remarks.

II. Calculation Procedure

All the geometries of reactants, intermediates, and transition states have been optimized by the gradient technique with the second order Møller–Plesset perturbation (MP2) method. For the Rh atom the 4s4p4d5s electrons are explicitly considered with the relativistic effective core potential (RECP), ECP17, and the standard (5s5p4d/3s3p2d) basis set.[9] For the P and Cl atoms only the valence 3s3p shells are explicitly considered with the ECP and the (3s3p/2s2p) basis set.[10] For other atoms the standard 6-31G basis set[11] is employed. The Gaussian92 program[12] has been used.

The structure and stability of the active catalytic species $RhCl(PH_3)_2$ has been studied in detail by Koga and Morokuma.[13] In general, it has been found that (1) using the notation of Chart 1, the ground state of this d^8 complex is a triplet $^3A_1[(b_1)^2(a_2)^2(b_2)^2(a_1)^1(a_1)^1]$, followed by the closed shell singlet $^1A_1[(b_1)^2(a_2)^2(b_2)^2(a_1)^2]$, and the open shell singlet $^1A_1[(b_1)^2(a_2)^2(b_2)^2(a_1)^1(a_1)^1]$, in the order of increasing energy within a range of 15 kcal/mol or so; (2) in the triplet state the Rh–Cl and Rh–P bonds are longer by 0.1 Å than in the closed shell singlet; (3) the use of the effective core potential, ECP9, where only 4d5s electrons but not 4s4p electrons are explicitly considered for Rh atom, overestimates the electron correlation energy; and (4) the ECP17 tends to give the Rh–ligand bonds too long by 0.03–0.08 Å.

The geometry optimization for $RhCl(PH_3)_2$ (**a0**) carried out in this paper at the MP2 level under the C_s symmetry constraint, gave the C_{2v} structure with the Rh–Cl, Rh–P, and P–H bond lengths of 2.384, 2.394, and 1.418 Å, respectively, and with the bond angle ∠ClRhP of 86.9°, which are in good agreement with those obtained by Koga and Morokuma[13] at the RHF level with the similar basis sets.[13]

As pointed out by Koga and Morokuma,[13] we expect that the closed shell singlet state becomes the ground state as soon as $RhCl(PH_3)_2$ interacts with other ligands and also in the d^6-RhL_5 complex, as illustrated in Chart 1. Therefore, we study only the overally singlet state for the present olefin hydroboration reactions.

Table 1. Energies[a] (at the MP2 Level) for Reactants, Intermediates, Transition States, and Products of the Reaction $RhCl(PH_3)_2 + HBR + C_2H_4$

species[b]	R = $(OH)_2$ **a**	R = $O_2(CH_2)_3$ **b**
$RhCl(PH_3)_2$	*−139.77794*	
HBR	*−176.47352*	*−292.59408*
C_2H_4	*−78.18420*	
C_2H_5BR	*−254.70845*	*−370.83236*
$RhCl(PH_3)_2 + HBR + C_2H_4$, **0**	0.0	0.0
$RhCl(PH_3)_2HBR + C_2H_4$, **1**	−47.1	−15.6
2, EQ	−47.2	−48.9
3, TS	−40.7	
4, TS for CH_3 rot.	−75.3	
5, EQ	−76.5	
6, second order top	−27.6	
7, TS	−29.8	
$RhCl(PH_3)_2 + C_2H_5BR$, **8**, EQ	−31.8	−33.9
9, TS	−46.6	−42.9
10, TS for $B(OH)_2$ rot.	−66.8	−69.4
10′, EQ	−67.8	
11, TS for $CH_2B(OH)_2$ rot.	−60.0	
12, TS	−45.4	−48.6
12′, second order top	−31.2	
13, second order top	−40.0	
14, TS for $B(OH)_2$ rot.	−48.5	−51.6
14′, EQ	−52.6	
15, TS for $CH_2B(OH)_2$ rot.	−44.0	
16, EQ	−71.0	
17, TS	−14.5	
18	−66.1	
19, EQ	−67.1	
20, TS	−29.5	
21, EQ	−55.0	
$RhCl(PH_3)_2C_2H_4 + HBR$, **22**, EQ	−53.4	−53.4

[a] Total energies (italic, in hartree) are given only for reactants, products, and reference structures and relative energies (in kcal/mol) are given for other structures. [b] Frequency analysis has not been performed, and the estimated number of imaginary frequencies based on comparison of energies for different conformations (see text for more details).

III. Catalytic Hydroboration of C_2H_4 by $HB(OH)_2$

In this section we consider the catalytic reaction:

$$RhCl(PH_3)_2 + HB(OH)_2 + C_2H_4 \rightarrow RhCl(PH_3)_2 + C_2H_5B(OH)_2 \quad (1)$$

The substrate $HB(OH)_2$ is a realistic model of borane having oxygen ligands for the experimental catecholborane (CB) or 4,4,6-trimethyl-1,3,2-dioxaborinane (TMDB). The first step of the catalytic cycle, after the active catalytic species $RhCl(PH_3)_2$ is generated, should be the addition of either (**I**) borane or (**II**) C_2H_4 to the active catalyst. We consider these two mechanisms separately.

Mechanism I: Initial Addition of Borane. At first we will examine the mechanism in which borane makes the first addition to the active catalyst. After the oxidative addition of the borane to the active catalyst, C_2H_4 can, in principle, coordinate to the

(9) Hay, P. J.; Wadt, W. R. *J. Chem. Phys.* **1985**, *82*, 299.
(10) Wadt, W. R.; Hay, P. J. *J. Chem. Phys.* **1985**, *82*, 284.
(11) (a) Hariharan, P. C.; Pople, J. A. *Theor. Chim. Acta* **1973**, *28*, 213. (b) Francl, M. M.; Pietro, W. J.; Henre, W. J.; Binkley, J. S.; Gordon, M. S.; DeFrees, D. J.; Pople, J. A. *J. Chem. Phys.* **1982**, *77*, 3654.
(12) *GAUSSIAN 92*; Fresch, M. J.; Trucks, G. W.; Head-Gordon, M.; Gill, P. M. W.; Wong, M. W.; Foresman, J. B.; Johnson, B. G.; Schlegel, H. B.; Robb, M. A.; Replogle, E. S.; Gomperts, R.; Andres, J. L.; Raghavachari, K.; Binkley, J. S.; Gonzales, C.; Martin, R. L.; Fox, D. J.; DeFrees, D. J.; Baker, J.; Stewart, J. J. P.; Pople, J. A.; Gaussian Inc., Pittsburgh, PA, 1992.
(13) Koga, N.; Morokuma, K. *J. Phys. Chem.* **1990**, *94*, 5454.

Table 2. MP2 Optimized Geometries (Distances in Å, Angles in deg) for Reactants, Intermediates, Transition States, and Products of the Reaction $RhCl(PH_3)_2 + HBR + C_2H_4 \rightarrow RhCl(PH_3)_2 + C_2H_5BR$ (Where R = $(OH)_2$ and $O_2(CH_2)_3$)

	RhCl	RhP	ClRhP	RhH	RhB	BH	ClRhH	ClRhB	BO	OBO	RhC^1	RhC^2	C^1RhC^2	C^1C^2	C^1H	C^2B	HRhC	BRhC
a0	2.384	2.394	86.9			1.185			1.399	121.4				1.351				
a1	2.448	2.369	89.4	1.583	2.056	1.995	147.7	147.2	1.423	118.9								
	2.418	*2.338*	*87.8*		*1.961*			*137.5*	*1.430*	*107.9*[a]								
a2	2.471	2.339	86.8	1.690	2.142		85.4	80.8	1.422	120.0	2.124	2.161	40.0	1.467	2.520	2.527	81.9	71.9
a3	2.474	2.339	86.0	1.735	2.110		90.4	89.4	1.425	118.5	2.218	2.135	39.3	1.467	1.782	2.975	51.9	89.0
a4	2.478	2.359	89.1	2.544	2.013		94.8	127.7	1.424	119.9	2.816	2.112	33.0	1.552	1.108	2.692	23.1	81.4
a5	2.474	2.357	89.1		2.015		128.0	128.1	1.423	120.1	2.897	2.125	31.2	1.542	1.104	2.633	6.3	78.9
a6	2.419	2.363	86.4	2.396	2.207		107.1	140.5	1.424	123.7	2.707	2.163	36.4	1.607	1.099	1.920	23.9	52.1
a7	2.418	2.363	86.3		2.198		137.8	140.5	1.424	123.7	2.748	2.170	35.2	1.587	1.103	1.919	5.7	52.1
a8	2.384	2.394	86.9						1.409	123.0				1.560	1.099	1.577		
a9	2.506	2.346	87.5	1.652	2.151		84.4	79.5	1.419	121.6	2.110	2.213	40.2	1.489	2.861	2.106	98.3	57.7
a10	2.501	2.361	90.4	1.569	2.845		142.7	82.7	1.408	124.1	2.152	2.987	30.2	1.562	2.263	1.586	73.0	31.4
a10′	2.556	2.355	88.8	1.568	3.066		106.6	107.4	1.411	123.5	2.113	3.022	29.3	1.569	2.553	1.587	86.5	30.2
a11	2.484	2.360	89.9	1.577			147.1	116.9	1.406	123.8	2.128	2.920	31.0	1.549	2.267	1.582	73.8	8.8
a12	2.417	2.364	88.2	1.634	2.721		163.5	96.0	1.416	123.0	2.285	2.897	33.2	1.588	1.324	1.591	34.7	32.7
a12′	2.428	2.358	87.0	1.640	3.219		158.7	112.6	1.396	123.0	2.381	3.106	29.9	1.581	1.254	1.590	29.7	29.0
a13	2.413	2.360	87.2	1.624			160.0	138.6	1.407	123.7	2.287	2.885	32.8	1.570	1.345	1.582	35.3	6.5
a14	2.393	2.375	87.4	1.798	2.907		176.9	110.7	1.413	123.6	2.752	3.299	28.3	1.570	1.126	1.589	15.4	28.8
a14′	2.400	2.380	87.2	2.227	3.511		118.3	193.2	1.436	118.9	3.319	3.981	22.5	1.565	1.099	1.580	2.7	23.3
a15	2.395	2.375	86.5	1.830			168.0	140.4	1.406	123.8	2.690	3.085	30.3	1.559	1.134	1.582	19.2	3.1
a16	2.522	2.347	91.0	1.598	2.062	2.412		86.2	1.419	119.3	2.450	2.427	32.9	1.382	2.660		79.1	
a17	2.428	2.378	88.1	1.972	2.253	1.574		80.7	1.415	123.1	2.355	2.146	38.6	1.499	1.394		36.2	
a18	2.474	2.368	88.9	3.308	2.002	2.417		110.1	1.421	120.0	3.285	2.141	23.0	1.557	1.095		19.1	
a19	2.540	2.342	89.4	1.597	2.059	2.359	86.3		1.424	118.9	2.311	2.339	35.0	1.400		2.787		78.4
a20	2.453	2.353	91.0	1.639	2.353	2.301	133.9		1.428	121.2	2.252	2.555	34.7	1.464		1.807		43.0
a21	2.497	2.371	86.5	1.575	3.335	2.342	173.5		1.410	123.8	2.158	3.229	24.4	1.546		1.580		27.8
a22	2.425	2.358	87.5			1.197			1.197	120.0	2.132	2.132	38.8	1.452				
b0	2.384	2.394	86.9			1.189			1.392	123.1				1.351				
b1	2.487	2.400	91.0	1.609	2.050	2.155	165.0	124.0	1.402	121.2								
b2	2.475	2.337	87.0	1.691	2.142		85.6	79.7	1.409	120.6	2.122	2.161	40.1	1.469	2.556	2.501	83.5	71.1
b9	2.568	2.401	86.6	1.610	2.189		84.4	80.8	1.401	121.7	2.100	2.249	40.1	1.497	2.857	2.047	99.8	54.9
b10	2.502	2.360	90.1	1.564	2.842		133.1	90.7	1.399	122.6	2.139	2.959	30.5	1.558	2.273	1.593	73.9	31.8
b12	2.421	2.361	88.2	1.629	2.728		160.5	98.9	1.405	122.4	2.286	2.902	32.9	1.585	1.332	1.595	34.9	32.7
b14	2.396	2.374	88.1	1.784	2.865		174.7	109.2	1.403	122.7	2.700	3.224	29.1	1.570	1.131	1.594	17.4	29.6
b8	2.384	2.394	86.9						1.410	119.3				1.560	1.099	1.580		

[a] Experimental results were given in italics for $RhHCl(Bcat)(PPr^i_3)_2$.[3v]

complex from three different directions: (**I.1**) between B and H ligands, *trans* to the Cl atom, (**I.2**) between H and Cl atoms, *trans* to B, and (**I.3**) between B and Cl atoms, *trans* to H. In the case **I.1**, the reaction can proceed via two distinct pathways: (**I.1.A**) insertion of C=C into the Rh−H bond followed by reductive elimination of $CH_3CH_2B(OH)_2$ by coupling of CH_2-CH_3 and $B(OH)_2$ and (**I.1.B**) insertion of C=C into the Rh−B bond followed by reductive elimination of $CH_3CH_2B(OH)_2$ by coupling of $CH_2CH_2B(OH)_2$ and H. In the path **I.2**, the C=C bond has to insert first into the neighboring Rh−H bond, and isomerization of the intermediate complex is necessary for further reductive elimination of $CH_3CH_2B(OH)_2$ by coupling of CH_2CH_3 and $B(OH)_2$. In the path **I.3**, only the Rh−B bond is available for insertion of C=C, followed by isomerization of the intermediate and subsequent reductive elimination by coupling of $CH_2CH_2B(OH)_2$ and H.

Thus, we have to consider four different mechanisms of the reaction (1) after oxidative addition of the borane to the active catalyst. Energies and geometries for the reactants, intermediates, transition states (TSs), and products of the reaction (**a0**−**a21**) are shown in Tables 1 and 2, respectively. The species through the mechanism **I.1.A** (**a0**−**a8**) are illustrated in Figure 1, and those for the mechanism **I.1.B** (**a1, a9**−**a15, a8**) are shown in Figure 2. The intermediates and transition states for the mechanism **I.2** (**a16**−**a18**) and **I.3** (**a19**−**a21**) are presented in Figure 3. The overall profiles of the potential energy surfaces (PESs) for all these mechanisms are shown in Figure 4.

Oxidative Addition of $HB(OH)_2$ to $RhCl(PH_3)2$. The calculation showed the oxidative addition to occur without any activation barrier. Despite careful search, we could not find the coordination complex, $RhCl(PH_3)_2[HB(OH)_2]$, where the B−H bond is preserved and the $HB(OH)_2$ ligand occupies a single coordination site. One can safely say that breakage of the B−H bond and formation of Rh−H and Rh−B bonds occur without barrier. In the experimental situation, the active catalyst is actually solvated and stabilized, and an energy of desolvating may give rise to an activation barrier.

We have found only one oxidative addition product, $RhHCl[B(OH)_2](PH_3)_2$, (**a1**) as shown in Figure 1. Geometry of **a1** was optimized without any symmetry constraint and converged to C_s symmetry, with Rh, Cl, B, and H atoms on the symmetry plane, while OH and PH_3 groups are reflected by this plane. The Rh atom in **a1** has a nearly trigonal bipyramidal environment, with two axial phosphines and equatorial Cl, H, and $B(OH)_2$. Optimization under C_s symmetry constraint starting with equatorial phosphines converged to the structure (**a1**) and the addition to give equatorial phosphines cannot take place. Since **a1** has C_s symmetry, we perform optimization of all other structures within C_s symmetry unless otherwise mentioned. Two equatorial bond angles, ∠ClRhH and ∠ClRhB, are about 147°, while the third, ∠BRhH, is much smaller, 65°; the equatorial ligands are Y-shaped, with Cl at the bottom of "Y". For a d^8 five-coordinate complex, the Y-shaped equatorial structure with the single poorest donor at the bottom of "Y" is in general preferred,[14] and the present result is consistent with this trend. The calculated structure of **a1** can be compared with the experimental X-ray structure of $RhHCl(Bcat)(PPr^i_3)_2$.[3v] As shown in Table 2, the agreement is satisfactory; the difference in Rh−Cl, Rh−P, and B−O distances is about 0.03 Å, the Rh−B bond length is 0.09 Å longer than the experiment, and

(14) Daniel, C.; Koga, N.; Han, J.; Fu, X. Y.; Morokuma, K. *J. Am. Chem. Soc.* **1988**, *110*, 3773.

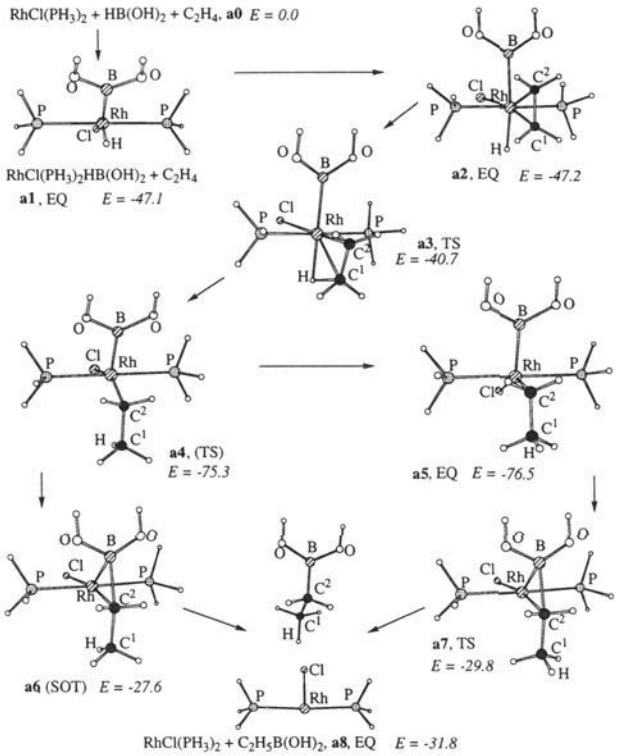

Figure 1. The critical structures of the **I.1.A** mechanism of the reaction $HB(OH)_2 + C_2H_4 + ClRh(PH_3)_2 \rightarrow ClRh(PH_3)_2 + C_2H_5B(OH)_2$. EQ, TS, and SOT stand for equilibrium, transition state, and second order top geometries, with parentheses indicating that one of the estimated imaginary frequencies is not related to the reaction.

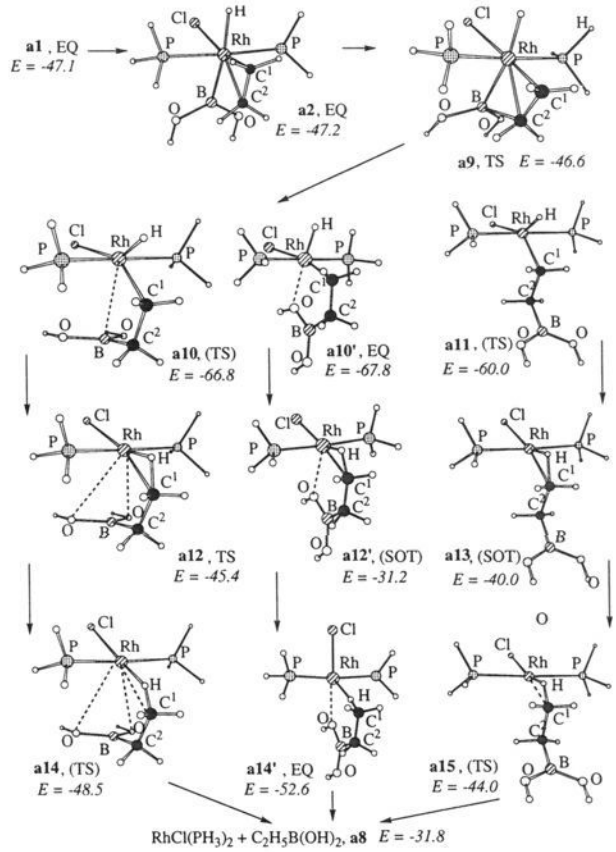

Figure 2. The critical structures of the **I.1.B** mechanism of the reaction $HB(OH)_2 + C_2H_4 + ClRh(PH_3)_2 \rightarrow ClRh(PH_3)_2 + C_2H_5B(OH)_2$. See Figure 1 for notation.

calculated and observed ∠PRhCl angles differ only by about 1°. Our ∠ClRhB angle is 10° larger than the experiment; we do not know at the moment the reason for this discrepancy.

The exothermicity of the oxidative addition of $HB(OH)_2$ to $RhCl(PH_3)_2$ is calculated to be 47.1 kcal/mol at the MP2/I// MP2/I level. However, this number might be overestimated by several kcal/mol because of basis set superposition error.[15-17]

Mechanism I.1.A. Coordination of ethylene to Rh(H)Cl-$(PH_3)_2[B(OH)_2]$ (**a1**) between H and $B(OH)_2$ ligands gives the complex $Rh(H)Cl(PH_3)_2[B(OH)_2](C_2H_4)$ (**a2**). The rhodium atom in **a2** is six-coordinated and has nearly an octahedral environment. The ∠ClRhB and ∠ClRhH angles are reduced to 80.8° and 85.4°, respectively, and ∠BRhX and ∠HRhX angles, where X is the center of the C=C bond, are in the range of 90−100°. The Rh−H and Rh−B bond lengths are elongated by about 0.1 Å, relative to **a1**. The C−C bond is 1.467 Å, stretched by 0.12 Å as compared to the free C_2H_4 molecule and close to those in metallocycle structures.[18] The $Rh-C^1$ and $Rh-C^2$ distances are 2.124 and 2.161 Å, respectively, which also are close to those for Rh−C covalent bond.[18] Thus, **a2** has a metallocycle structure.

The binding energy $Rh(H)Cl(PH_3)_2[B(OH)_2](C_2H_4)$ (**a2**) → $Rh(H)Cl(PH_3)_2[B(OH)_2] + C_2H_4$ is calculated to be only 0.1 kcal/mol, a surprising small value. The reason of this is that the attack of the C_2H_4 to **a1** between H and $B(OH)_2$ ligands is highly unfavorable. In order to find the origin of the small binding energy, we divide this binding energy ΔE into three parts:

$$\Delta E = \mathrm{DEF}(\mathbf{a1}) + \mathrm{DEF}(C_2H_4) + \mathrm{INT} \qquad (2)$$

DEFs are energies required to deform the reactant fragments, **a1** and C_2H_4, from their respective equilibrium geometries to the geometries in the product complex **a2**. INT is the interaction energy between the deformed fragments. Table 3 shows that the energy required to open the narrowest angle of Y to make it a T shape is extremely large (66 kcal/mol), compared to those required to open the wider angle fo Y to make a T to be discussed later with the product **a16** and **a19**. Since the product **a2** is a metallocycle, the interaction energy INT is large in magnitude but cannot compensate the large DEF.

The reaction proceeds further via migratory insertion of the C=C bond into the Rh−H bond through TS (**a3**), which is an early transition state, in accord with high exothermicity of the **a2** → **a3** → **a4** process. Table 2 shows that the Rh−H bond in **a3** is only 0.045 Å longer than in **a2**, and the C−C distance has not changed. Although the C^1-H distance in **a3** is 0.7 Å shorter than in **a2**, it is still very far from the regular C−H bond length. The $Rh-C^1$ distance is lengthened by about 0.1 to 2.22 Å in **a3**, but the bond is still preserved in the TS. Geometry of the reacting fragment has a double three-centered character, with H, C^1, and C^2 all interacting with Rh. The barrier height is 6.5 kcal/mol relative to **a2**, and **a3** lies substantially below the initial reactants, $RhCl(PH_3)_2 + HB(OH)_2 + C_2H_4$ (**a0**).

Insertion maintaining C_s symmetry results in the complex **a4**, $RhCl(PH_3)_2[B(OH)_2](C_2H_5)$, which is 28.2 kcal/mol lower than

(15) (a) Morokuma, K.; Kitaura, K. *In Chemical Application of Atomic and Molecular Electrostatic Potentials*; Politzer, P., Truhler, D. G., Eds.; Plenium: New York, 1981. (b) Kitaura, K.; Sakaki, S.; Morokuma, K. *Inorg. Chem.* **1981**, *20*, 2292.

(16) Frish, M. J.; Del Bene, J. E.; Binkley, J. S.; Schaefer, III, H. F. *J. Chem. Phys.* **1986**, *84*, 2279.

(17) Koga, N.; Morokuma, K. *J. Am. Chem. Soc.* **1993**, *115*, 6883.

(18) Sodupe, M.; Bauschlicher Jr., C. W.; Langhoff, S. R.; Partridge, H. *J. Phys. Chem.* **1992**, *96*, 2118.

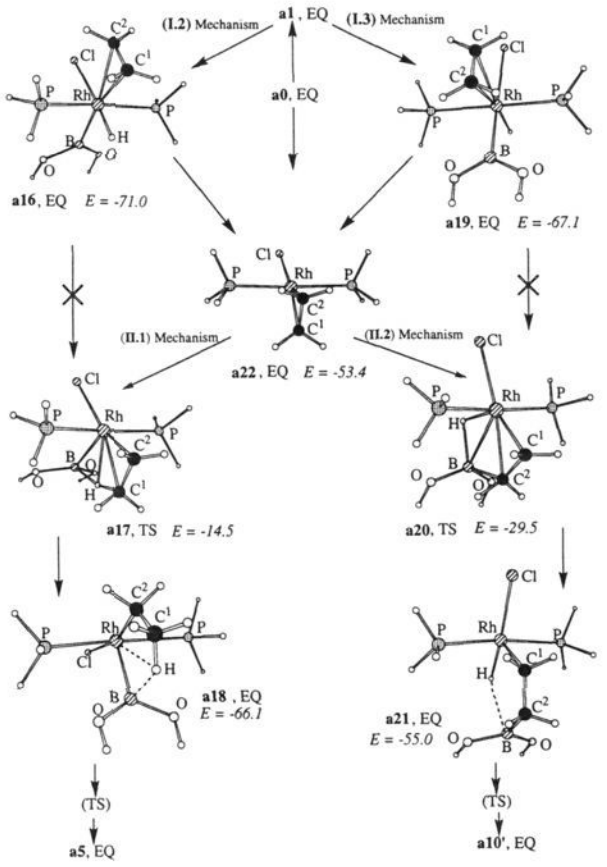

Figure 3. The critical structures of the **I.2** and **I.3** mechanisms of the reaction $HB(OH)_2 + C_2H_4 + ClRh(PH_3)_2 \rightarrow ClRh(PH_3)_2 + C_2H_5B(OH)_2$. See Figure 1 for notation.

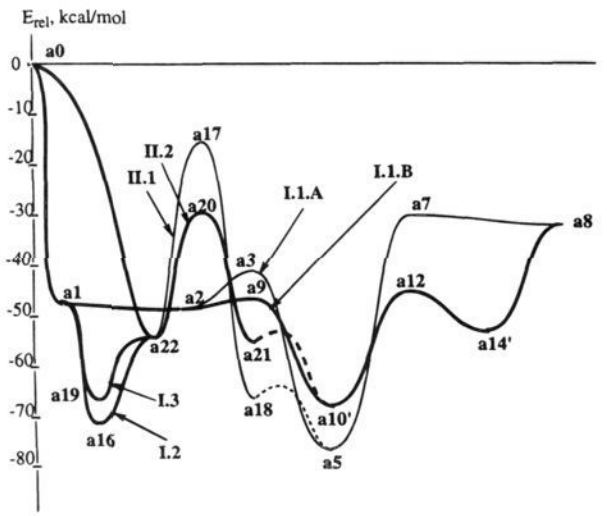

Figure 4. The overall profiles of the potential energy surface of the reaction $HB(OH)_2 + C_2H_4 + ClRh(PH_3)_2 \rightarrow ClRh(PH_3)_2 + C_2H_5B(OH)_2$. Labels such as **I.1.A** refer to different mechanisms, and labels such as **a1** refer to transition states and intermediates. The bold curves show the most favorable reaction mechanisms. The dashed curves mean that the transition states between **a21** and **a10'** and between **a18** and **a5** were not calculated, but the barriers are expected to be low.

a1. This energy difference is probably attributable to the fact that a Rh−C bond is stronger than a Rh−H bond. In **a4** the ethyl group has an eclipsed conformation, but no agostic interaction between a β-H atom and Rh is recognized. We have found that the staggered ethyl conformation (**a5**) of the complex within C_s symmetry is lower than **a4** by 1.2 kcal/mol. TS search

Table 3. Energy Decomposition Analysis of the **a2**, **a16**, **a19**, and **b2** Complexes[a]

	DEF				
structure	C_2H_4	$RhCl(PH_3)_2(H)BR$	total	INT	ΔE
a2	7.5	66.1	73.6	−73.7	−0.1
a16	0.6	2.2	2.8	−26.6	−23.8
a19	1.5	10.2	11.7	−31.6	−19.9
b2	7.7	26.2	33.9	−67.2	−33.3

[a] Here all numbers are given in kcal/mol. DEF and INT are deformation and interaction energies, respectively. ΔE is a binding energy which is calculated as DEF + INT.

without symmetry converged to **a4**, and, therefore, **a4** is the TS for CH_3 rotation. Thus the reaction from **a2** should give the ethyl intermediate **a5** with the exothermicity of 29.3 kcal/mol. Geometries of **a4** and **a5** are very similar, except for the CH_3 torsion angle. In **a5** the metal atom is still five-coordinated, with equatorial Cl, B, and ethyl in a Y-shape with Cl at the bottom of the Y, as was the case in the hydride (**a1**). Compared to **a2**, the Rh−B distance in **a5** is shortened by 0.1 Å, suggesting the strengthening of the bond.

Both **a4** and **a5** can undergo reductive elimination of $C_2H_5B(OH)_2$ through the "TS" **a6** and **a7**, respectively, optimized within the C_s symmetry. The energy of **a7** is 2.2 kcal/mol lower than that of **a6**. Therefore, one can suggest **a7** to be a real TS, and **a6** to be a second order top with two imaginary frequencies, one for reaction and another for internal rotation of CH_3. **a7** is a three-center TS, with Rh, B, and C^2 forming a triangle with the sides of 1.92 (C^2−B), 2.17 (Rh−C^2), and 2.20 (Rh−B) Å. Beyond the transition state, the process reproduces the initial active catalyst, unsaturated $RhCl(PH_3)_2$, and the reaction product $C_2H_5B(OH)_2$ (**a8**). The barrier for the reductive elimination is calculated to be very high, 46.7 kcal/mol, reflecting the large endothermicity of 44.7 kcal/mol of the final step, **a5** → **a7** → **a8**. The exothermicity of the overall reaction $HB(OH)_2 + C_2H_4 \rightarrow C_2H_5B(OH)_2$ reaction is calculated to be a 31.8 kcal/mol. The reverse reaction of the product $C_2H_5B(OH)_2$ with the free active catalyst $RhCl(PH_3)_2$ to give the stable intermediate **a5** has a barrier of only 2 kcal/mol; however, the active catalyst is actually solvated, and the barrier from the solvated catalyst to the TS (**a7**) could be substantial.

Thus, the reductive elimination of $C_2H_5B(OH)_2$ is the rate-determining step for **I.A** mechanism. The barrier seem to be too high for the reaction to occur via this mechanism at low temperatures.

Mechanism I.1.B. As shown in Figure 2, mechanism **I.1.B** starts with migratory insertion of the olefin into the Rh−B bond in the olefin complex **a2**, leading to the intermediate $Rh(H)Cl(PH_3)_2[CH_2CH_2B(OH)_2]$, for which different structures will be discussed below. The exothermicity of the insertion process is about 20 kcal/mol, and the activation barrier at the TS (**a9**) is very small, 0.6 kcal/mol. TS (**a9**), like (**a3**), has a double three-centered reaction center, with Rh, two C atoms, and B forming two triangles with the common side, Rh−C^2, which is still short, 2.21 Å. The C^1−C^2 distance in **a9** is slightly longer than in **a3**, and the C^2−B distance in **a9** is closer to the normal bond length than the C−H distance in **a3**. Therefore, **a9** is a later TS, relative to **a3**, in accord with the smaller exothermicity of insertion. TS **a9** may also be compared with **a7**, both being TSs for breakage of a Rh−B and formation of a C−B bond. The process **a2** → **a9** → **a10** is exothermic, while **a5** → **a7** → **a8** is endothermic. Consistent with this difference, **a9** is an earlier TS than **a7**; in **a9** the C^2−B distance is 0.09 Å longer and the Rh−B bond is 0.05 Å shorter than in **a7**. The barrier for C=C insertion into the Rh−B bond is significantly lower than that into the Rh−H bond.

We have obtained three different optimized structures of Rh(H)Cl(PH_3)$_2$[$CH_2CH_2B(OH)_2$] within C_s symmetry. The structure **a10** has an eclipsed C^1-C^2 bond with the boron atom *syn* to Rh at the Rh−B distance of 2.845 Å, and OH groups are out of the symmetry plane. In the structure **a10′**, the C^1-C^2 bond is eclipsed, and the entire $B(OH)_2$ fragment is on the symmetry plane, with the Rh−B distance of 3.07 Å. One of the oxygen atoms coordinates strongly with the Rh−O distance of 2.26 Å. The structure **a11** has a staggered C−C bond with the B atom *anti* to Rh. **a10′** is the most stable structure of the three, presumably due to the interaction between Rh and O. **a10** is 1 kcal/mol higher than **a10′** and is likely to have one imaginary frequency corresponding to rotation of the $B(OH)_2$ fragment around the C^2-B bond. **a11** lies 7.8 kcal/mol above **a10′** and is expected to have at least one imaginary frequency corresponding to rotation around the C^1-C^2 axis. The intermediates **a10′** and **a10** have ∠HRhC^1 of less than 90° and seem to be ready for dehydrogenative reductive elimination or coupling between $CH_2CH_2B(OH)_2$ and H.

Corresponding to three intermediates, three structures differing by position of $B(OH)_2$ have been found for the reductive elimination TS. The TS (**a12**) with *syn* B and out-of-plane $B(OH)_2$ is the most favorable, with the barrier of 22.4 kcal/mol from **a10′**. In spite of possibility of the Rh−O interaction with in-plane $B(OH)_2$, **a12′** is 14.2 kcal/mol higher in energy than **a12**. This may be due to the strain of a planar six-membered ring formed by Rh, H, C^1, C^2, B, and O atoms in **a12′**. Therefore, we performed calculations of the transition state without symmetry, starting from the geometry of slightly distorted **a12′**. The optimization converged to **a12**. This confirms **a12** to be a real transition state. **a13** with *anti* $B(OH)_2$ group is 5.4 kcal/mol above **a12**. **a12** is a transition state for insertion into the Rh−H bond but is later than **a3**. Rh−H and Rh−C distances are elongated with respect to those in **a10′** by 0.07 and 0.17 Å, respectively, and the C−H distance, 1.32 Å, is much shorter than that in **a3**, 1.78 Å. This is not surprising, since the **a2** → **a3** → **a5** reaction is exothermic, while the **a10′** → **a12** → **a14′** reaction is endothermic.

The TS (**a12**) leads to the product complex RhCl(PH_3)$_2$·[$C_2H_5B(OH)_2$]. Again, we have considered three different structures of this complex, **a14**, **a14′**, and **a15**, among which **a14′** with in-plane $B(OH)_2$ is the most favorable and lies 52.6 kcal/mol lower than the reactants. The complex is stabilized by the Rh−O interaction at the Rh−O distance of 2.33 Å. **a14** with out-of-plane $B(OH)_2$ is a 4.1 kcal/mol higher than **a14′**, and **a15** with B atom in *anti* position is 8.6 kcal/mol less favorable than **a14′**. Thus, we expect **a14′** to be a real local minimum for the product complex. The Rh−H distance in **a14** and **a15** is in the 1.8 Å range, much shorter than 2.3 Å in **a14′**, suggesting that these complexes are stabilized by the interaction of the agostic C−H bond with Rh. In going from TS (**a12**), at first the Rh−C^1 bond is broken and Rh−H is elongated from 1.63 to 1.80 Å, in the structure **a14**. Then, rotation of $B(OH)_2$ group leads to further weakening of the Rh−H bond and formation of the Rh···O chelate bond, while the energy is lowered by 4.1 kcal/mol to reach **a14′**.

a14′ dissociates into RhCl(PH_3)$_2$ + $C_2H_5B(OH)_2$ (**a8**) with energy loss of 20.8 kcal/mol but without a barrier. Because the active catalyst would be solvated, this energy loss would actually be lower. The overall pathway for the mechanism **I.B** is **a0** → **a1** → **a2** → **a9** → **a10′** → **a12** → **a14′** → **a8**. The rate-determining step is the reductive elimination of $C_2H_5B(OH)_2$ from the alkylhydrido complex, with the activation energy of 22.4 kcal/mol. As will be discussed later, this mechanism turns out to be the most favorable path of reaction 1.

Mechanism I.2. Mechanism **I.2** initiates by coordination of C_2H_4 to **a1** at the *trans* position of the boron atom, *cis* to the Cl and H atoms. As shown in Figure 3, the coordination complex formed (**a16**) is stabilized by 23.9 kcal/mol relative to **a1**, much lower in energy than the similar coordination complex **a2**. This large difference in the thermodynamic stability between **a16** and **a2** structures comes from the differences in the deformation energy (DEF) of the starting **a1** complex to form **a16**. As seen in Table 3, the DEF needed to "prepare" geometries of the reactant fragments **a1** and C_2H_4 is 2.8 kcal/mol, which is much less than that to form **a2**, 73.6 kcal/mol. Opening a wide side angle of a "Y" to form a "T" requires much less energy than opening a narrow top angle of a "Y". In **a16** the C−C distance changes little as compared to that in the free C_2H_4 molecule, the elongation being only 0.03 Å. Meanwhile, the Rh−C bond lengths are about 0.3 Å longer than those in **a2**. Thus, **a16** is a π-complex. Our attempts to find a metallocycle structure like **a2** have failed; optimization starting from a metallocycle structure converged to the π-complex without barrier. The Rh−H and Rh−B distances are significantly shorter in **a16** than those in **a2**.

The catalytic reaction could proceed from **a16** by migratory insertion of C=C into the Rh−H bond. The calculated transition state (**a17**) has an unexpected structure; the five atoms on the reaction site form three triangles, RhC^2C^1, RhC^1H, and RhBH. Both Rh−H and B−H distances, 1.97 and 1.57 Å, respectively, are short enough for strong interaction. Judging from the 0.4 Å shorter C^1−H bond length being formed, **a17** is a later transition state than **a3**. The Rh−C^1 bond length is still short, 2.36 Å, even shorter than that in **a16**, but longer than that in **a3**. The calculated barrier is very high, 56.5 kcal/mol relative to **a16**. After clearing the barrier **a17**, the system comes to the RhCl(PH_3)$_2$B(OH)$_2$(C_2H_5) complex (**a18**) which is 4.9 kcal/mol higher than **a16** and 10.4 kcal/mol above **a5**. In going from **a16** to **a18** via the transition state (**a17**) the Rh−H and Rh−C^1 bonds are broken, and the C^1−H bond is created. However, the geometry of **a17** suggests this transition state to correspond to a pathway of "σ-bond metathesis", involving coordination of C_2H_4 to the metal center followed by coordination of $HB(OH)_2$ to the complex and simultaneous cleavage of the coordination Rh−C^1 bond and the B−H bond with formation of the Rh−B and C−H bonds. **a17** looks like a five-center transition state. However, the Rh−C^2 bond is preserved as in **a16** and **a17**, as in the **a18** product. Therefore, one can say that **a17** is a four-center (Rh, C^1, H, B) transition state, similar to the transition state of σ-bond metathesis in the CpRu(PPh_3)$_2$-Me + HBcat → CpRu(PPh_3)$_2$H + MeBcat reaction.[8] The barrier, calculated with respect to RhCl(PH_3)$_2$(C_2H_4) + $HB(OH)_2$ (**a22**), is 39.5 kcal/mol.

To confirm to what structure the transition state **a17** is connected, **a16** or **a22**, we have performed quasi-IRC calculations, optimization of geometry down from **a17** using estimated force constants of the transition state and following the eigenvector that corresponds to the imaginary frequency. The calculation leads to dissociation of $HB(OH)_2$. Therefore, **a17** is connected with **a22**, RhCl(PH_3)$_2$(C_2H_4) + $HB(OH)_2$, but not with **a16**, and it is indeed the transition state for σ-bond metathesis.

The transition structure **a17** is very much (26.2 kcal/mol) higher than **a3**. We tried to find another transition state with lower energy for the mechanism **I.2**, which is similar to **a3** and connected with **a16** and corresponds to the insertion into Rh−H bond. We used **a3** with the position of Cl and $B(OH)_2$ exchanged as the initial guess for TS optimization. The energy of this structure is even slightly lower than the energy of **a3**.

However the TS optimization converged to **a17**. An explanation can be given by comparison of the resulting complexes **a4** and **a18**. The five-coordinated complex **a4** is "Y"-shaped with the poorest donor Cl at the bottom of "Y", with the equatorial $ClRhC^2$, $BRhC^2$, and ClRhB angles of 150.9°, 81.4°, and 127.7°, respectively. As discussed above and previously,[14] this is the most stable structure, and those structures with Cl on a top arm of Y are, in general, very unstable. For instance, the complex **a4** with switched Cl and $B(OH)_2$ is 49.3 kcal/mol higher than **a4** and, also, 40.1 kcal/mol higher than **a18**. Thus, in the optimized structure **a18** Cl tries to be at the bottom arm of Y, with the $ClRhC^2$ and $BRhC^2$ angles of 161.3° and 88.6°, respectively. This small $BRhC^2$ angle in **a18** forces the ethyl and $B(OH)_2$ groups to be uncomfortably close to each other, for instance with the B−H distance 2.42 Å. The endothermicity of the **a16** → **a18** step would give a late character to the transition state between them. As a result, the transition state would suffer from the same structural difficulties as **a18** does, and the calculated high energy TS (**a17**) is not even connected to **a16**. Thus, to get from **a16** to **a18**, the system first has to dissociate $HB(OH)_2$ leading to **a22**. Then, σ-bond metathesis occurs, via the transition state **a17**. The process of $HB(OH)_2$ reductive elimination from **a16** is endothermic by 17.6 kcal/mol. We tried to find an elimination barrier. However, the TS optimization converged to **a22**. Apparently, the reverse process, oxidative addition of $HB(OH)_2$ to $RhCl(PH_3)_2(C_2H_4)$ has no activation energy, similar to the addition of $HB(OH)_2$ to $RhCl(PH_3)_2$.

Since the structure **a22**, $RhCl(PH_3)_2C_2H_4$, can be obtained directly by addition of olefin to the catalyst, mechanism **I.2** merges at this point with mechanism **II**, which will be discussed in one of the following sections.

Mechanism I.3. As shown in Figure 3, the initial complex for mechanism **I.3** is $RhCl(PH_3)_2(H)B(OH)_2(C_2H_4)$ (**a19**) where the C_2H_4 ligand is situated *trans* to the H atom, *cis* to Cl and B. The geometry of **a19** is in between but closer to that of **a16**, a π-complex, than that of **a3**, a metallocycle. The Rh−C distances are 0.1 Å shorter than those in **a16** and about 0.2 Å longer than those in **a3**. The C−C bond length is only 0.02 Å longer as compared to that in **a16**.

The next step is olefin migratory insertion into the Rh−B bond. The transition state (**a20**) for the process is similar to **a17**, a four-center TS with relatively short B−H and Rh−B distances of 2.30 and 2.35 Å, respectively. The transition state is late, where the C^2−B distance is only 1.81 Å, the shortest in all the TSs considered that form a C−B bond. Since geometry of **a20** is similar to that of **a17**, we presume that **a20** is a transition state for σ-bond metathesis process and is connected with **a22**. The barrier height is 23.9 kcal/mol. The reaction cannot proceed directly from **a19** to the transition state **a20**; instead, $HB(OH)_2$ reductive elimination has to take place to form $RhCl(PH_3)_2(C_2H_4)$ (**a22**), without barrier, as discussed in the preceding subsection. At this point mechanism **I.3** merges with mechanism **II**, which will be discussed in the next section.

Mechanism II: Initial Addition of Olefin. As was mentioned above, the initial step of reaction 1 via mechanism **II** is formation of $RhCl(PH_3)_2(C_2H_4)$ (**a22**), which is stable relative to reactants by 53.4 kcal/mol, as shown in Figure 3. The C−C bond in this complex is 1.452 Å, indicating a metallocycle structure. Upon coordination of $HB(OH)_2$ to **a22**, the reaction can proceed by various pathways. Oxidative addition of borane without barrier leads to the complexes **a16** or **a19** with energy gain of 17.6 and 13.7 kcal/mol, respectively. **a16** and **a19** can eliminate C_2H_4 losing 23.9 and 20.0 kcal/mol, respectively. After that, the complex **a1** is formed, and the reaction continues by mechanism **I**. Conversely, as discussed before, **a22** can be formed via pathway **I.2** and **I.3**.

If oxidative addition of borane to **a22** does not occur, σ-bond metathesis takes place, and two different pathways are possible. The pathway **II.1**, which goes through the transition state (**a17**) by cleavage of the B−H bond and formation of the C−H and Rh−B bonds, leads to the complex $RhCl(PH_3)_2[B(OH)_2][C_2H_5]$ (**a18**). The barrier height is 39.5 kcal/mol, relative to **a22**, and exothermicity of the metathesis process **a22** → **a18** is 7.7 kcal/mol. **a18** can be transformed to the more favorable isomer **a5** by 180° rotation of C_2H_5 fragment around the Rh−C^2 bond. The rotational barrier is calculated to be low for the related reaction $RhCl(PH_3)_2 + HBH_2 + C_2H_4$,[19] and therefore is not expected to be high for reaction 1. Afterward, **a5** can be connected via the transition state **a7** to the **a8** products.

Pathway **II.2**, occurring through the transition state **a20** by cleavage of the B−H bond and formation of the C−B and Rh−H bonds, results in the complex $RhCl(PH_3)_2(H)[C_2H_4B(OH)_2]$ (**a21**). The barrier is 23.9 kcal/mol, and exothermicity of the **a22** → **a21** step is 1.6 kcal/mol. **a21** is 12−13 kcal/mol higher than **a10** and **a10′** and can rearrange to the latter structures by rotation of the $C_2H_4B(OH)_2$ fragment around the Rh−C^1 axis. Though the barrier for rearrangements was not calculated, it is expected to be low. After the isomerization, the reaction would be completed by coupling of H and $C_2H_4B(OH)_2$, **a10′** → **a14′** via TS **a12**, and dissociation of $C_2H_5B(OH)_2$.

Comparison of Different Mechanisms. As can be confirmed in Figure 4, mechanism **I.1.B** has been found to be the most favorable pathway for the catalytic $RhCl(PH_3)_2 + C_2H_4 + HB(OH)_2 \rightarrow RhCl(PH_3)_2 + C_2H_5B(OH)_2$ reaction. It involves oxidative addition of $HB(OH)_2$ to $RhCl(PH_3)_2$ to give **a1**, coordination of C_2H_4 to the complex between H and B ligands to give (**a2**), insertion of C=C into the Rh−B bond via TS (**a9**) to give **a10′**, followed by coupling of H and $CH_2CH_2B(OH)_2$ or dehydrogenative reductive elimination of $CH_3CH_2B(OH)_2$ via TS (**a12**) to form the product complex $RhCl(PH_3)_2[C_2H_5B(OH)_2]$ (**a14′**) from which finally $C_2H_5B(OH)_2$ is dissociated. Though the final dissociation step requires 20.8 kcal/mol in the calculations, in solution the regenerated active catalyst is actually solvated and stabilized, and the net energy requirement should be smaller. Therefore, the rate-determining step is the coupling of H and $CH_2CH_2B(OH)_2$ with the activation energy of 22.4 kcal/mol via TS (**a12**). Mechanism **I.1.A**, where the insertion takes place to the Rh−H bond, is not facile due to a high barrier of 46.7 kcal/mol for the coupling of CH_3CH_2 and $B(OH)_2$ which is accompanied by immediate dissociation of $C_2H_5B(OH)_2$. The $RhCl(PH_3)_2HB(OH)_2(C_2H_4)$ complex with C_2H_4 between H and Cl ligands (**a16**) and between B and Cl ligands (**a19**) are much more stable than **a2** with C_2H_4 between B and H. However, transformations of **a16** and **a19** cannot occur by insertion into the Rh−H or the Rh−B bond but proceed through borane elimination and σ-bond metathesis processes.

If $RhCl(PH_3)_2(C_2H_4)$ (**a22**) complex is formed directly from **a0** or via $RhCl(PH_3)_2(H)B(OH)_2(C_2H_4)$ (**a16**) or (**a19**), the reaction could proceed via σ-bond metathesis pathway, and the barriers are 39.5 kcal/mol for mechanism **II.1** and 23.9 kcal/mol for mechanism **II.2**. Thus, mechanism **II.2** is more preferable than **II.1** and this barrier at TS (**a20**) is not much higher than the barrier 22.4 kcal/mol at TS (**a12**). Therefore, mechanism **II.2**, starting with C_2H_4 coordination and merging to mechanism **I.1.B** at **a10′**, might be able to compete with mechanism **I.1.B** starting with initial oxidative addition of

(19) Musaev, D. G.; Mebel, A. M.; Morokuma, K. to be published.

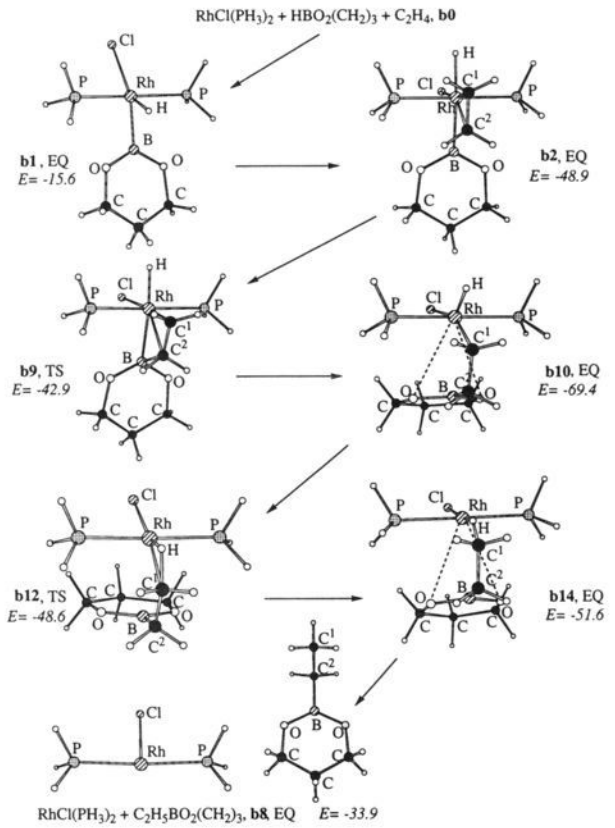

Figure 5. The critical structures of the **I.1.B** mechanism of the reaction $HBO_2(CH_2)_3 + C_2H_4 + ClRh(PH_3)_2 \rightarrow ClRh(PH_3)_2 + C_2H_5BO_2(CH_2)_3$. See Figure 1 for notation.

borane. In any case, during the catalytic cycle, initial formation of the C−B bond is superior to the formation of the C−H bond.

IV. Hydroboration of C_2H_4 by $HBO_2(CH_2)_3$

In this section we consider the catalytic reaction:

$$RhCl(PH_3)_2 + HBO_2(CH_2)_3 + C_2H_4 \rightarrow RhCl(PH_3)_2 + C_2H_5BO_2(CH_2)_3 \quad (3)$$

$HBO_2(CH_2)_3$ is a cyclic borane and a close analog of 4,4,6-trimethyl-1,3,2-dioxaborinane (TMDB) for which the catalytic hydroboration has been observed experimentally. For this reaction we have studied only mechanism **I.1.B**, which is the most favorable pathway for hydroboration with a model molecule $HB(OH)_2$. Our main purpose here is to compare the reaction energetics for the real molecule with that for the model system. Energies and geometries of various species are presented also in Tables 1 and 2, respectively. The intermediates and transition states for the reaction are drawn in Figure 5. We maintain the same notation as in the previous sections for corresponding structures with the letter "**b**" identifying the present system.

The first step of the reaction is oxidative addition of $HBO_2(CH_2)_3$ to $RhCl(PH_3)_2$ to form **b1**. As seen in Table 1 the geometries of **b1** and **a1** are similar, but **b1** has larger ∠ClRhH and ∠HRhB angles and a smaller ∠ClRhB angle. The B−H bond is broken, and, similar to the $B(OH)_2$ case, we have not found the complex with short B−H distance. Exothermicity of $HBO_2(CH_2)_3$ addition, 15.6 kcal/mol, is significantly smaller than that, 47.1 kcal/mol, for $HB(OH)_2$.

When the binding energies in **a1** and **b1** are divided into DEF and INT, as in eq 2, one finds that this large difference comes from the difference in the interaction energy: 87.6 kcal/mol between deformed $B(OH)_2$ and [Rh] fragment and 53.2 kcal/mol between deformed $BO_2(CH_2)_3$ and [Rh] fragment. Deformation energies of borane fragments are similar and negligibly small. Deformation energies of the [Rh] fragment in **a1** and **b1** are also close; the energy for **b1** is 1.9 kcal/mol lower than that for **a1**. Meanwhile, the H−B binding energies in the boranes themselves calculated at the MP2 level differ only by 3.2 kcal/mol: 104.2 and 101.0 kcal/mol for $HB(OH)_2$ and $HBO_2(CH_2)_3$, respectively. Thus, the strength of the forming Rh−B bond has to be very sensitive to the nature of ligands connected to the boron atom. The controversial question about the strength of the Rh−B interaction requires a separate careful study theoretically as well as experimentally.[20]

Coordination of C_2H_4 to **b1** between B and H atoms gives the metallocycle **b2**, which is geometrically very close to **a2**, with differences in bond lengths not exceeding 0.01 Å. Addition of C_2H_4 brings 33.3 kcal/mol of energy lowering, while the corresponding exothermicity for **a1** → **a2** is nearly zero. Table 3 shows that the origin of the difference is the much smaller (by 39.9 kcal/mol) deformation energy of $RhCl(PH_3)_2(H)BR$ fragment in **b2** than that in **a2**. Interestingly, in **b1** the ∠ClRhH and ∠ClRhB angles are 165.0° and 124.0°, and from **b1** to **b2** deformation of ∠ClRhH is larger than from **a1** to **a2**, while deformation of ∠ClRhB from **b1** to **b2** is smaller than from **a1** to **a2**. Therefore, the ∠ClRhB angle in the complex is significantly more rigid than ∠ClRhH, and deformation of the former is much more "expensive" energetically. Overall, the stability of **b2** with respect to **b0** is almost the same as stability **a2** with respect to **a0**.

The next reaction step, olefin insertion into Rh−B, occurs via the transition state (**b9**). While both **b9** and **a9** are early transition states reflecting similar exothermicity of this step between $HB(OH)_2$ and $HBO_2(CH_2)_3$ reactions, the transition state (**b9**) is slightly later than **a9**; the Rh−B distance is 0.04 Å longer, and C^2−B is 0.06 Å shorter in **b9**. The barrier for the insertion into Rh−B is 6.0 kcal/mol, compared to 0.6 kcal/mol for the $HB(OH)_2$ reaction. The transition state (**b9**) is sterically more congested than **a9** due to relatively short distances between hydrogens of C^2 and oxygens of the borane.

We have considered only one configuration for the $RhCl(PH_3)_2(H)[C_2H_4BO_2(CH_2)_3]$ complex **b10**, with B in *syn* position to Rh and the BO_2C_3 ring out of the symmetry plane. For $HB(OH)_2$ the in-plane **a10′** configuration was slightly more favorable, but the difference was not significant. Meanwhile, for the $BO_2(CH_2)_2$ complex, **b10′** is expected to be less favorable due to the steric factor. Hence, we have limited our consideration to only one configuration for this complex as well as for the transition state for the coupling of H and borylethyl and the product complex $RhCl(PH_3)_2[C_2H_5BO_2(CH_2)_3]$. **b10** is more stable than **b2** by 20.5 kcal/mol, similar to the difference 20.2 kcal/mol between **a10** and **a2**. Geometry of **b10** is very close to that of its analog **a10**.

b12 is the transition state for the coupling of H and $C_2H_4BO_2(CH_2)_3$ or the dehydrogenative reductive elimination and complexation of $C_2H_5BO_2(CH_2)_3$. The barrier 20.8 kcal/mol relative to **b10** is close to the corresponding value for $HB(OH)_2$ reaction. **b12** lies below the final reaction products, $RhCl(PH_3)_2 + C_2H_5BO_2(CH_2)_3$ (**b8**). Geometries of **b12** and **b14** have no large differences from those of **a12** and **a14**, except the 0.05 Å shorter Rh−C^1 distance in **b14** as compared to that in **a14**.

Finally, dissociation of $C_2H_5BO_2(CH_2)_3$ from **b14** leads to the products with the energy loss of 17.7 kcal/mol. Since a structure **b14′** with in-plane BO_2C_3 cycle and Rh−O bond might

(20) Rablin, P. R.; Hartwig, J. F.; Nolan, S. P. *J. Am. Chem. Soc.* **1994**, *116*, 4121.

be slightly more stable than **b14**, the endothermicity of the elimination process might be 3−4 kcal/mol higher. Anyway, the heat of this reaction step is comparable with that for the model $HB(OH)_2$ reaction. In solution, solvating of the regenerated active catalyst will lower this energy loss.

Thus, the entire reaction pathway, **b0** → **b1** → **b2** → **b9′** → **b10** → **b12** → **b14**, has the coupling of H and $C_2H_4BO_2(CH_2)_3$ as the rate determining step, with the activation energy of 20.8 kcal/mol. The profile of potential energy surface for the $HBO_2(CH_2)_3$ reaction is qualitatively and almost quantitatively the same as the profile of PES for the model reaction of $HB(OH)_2$, considered in the previous section. Therefore, our conclusions in the previous section and here can be extended to the hydroboration reactions with real boranes, such as HBcat or TMDB. Meanwhile, the steric factors for bulkier boranes could destabilize more compact structures, such as **b9** and **b10**, which would increase the small barrier for insertion into the Rh−B but would reduce the rate-determining barrier for the coupling of H and the borylethyl group.

V. Concluding Remarks

Mechanism **I.1.B** has been found to be the most favorable pathway of the catalytic hydroboration of C_2H_4 by $HB(OH)_2$ with the model Wilkinson catalyst, $RhCl(PH_3)_2$. Since the potential energy profile for the **I.1.B** mechanism for $HBO_2(CH_2)_3$ is nearly quantitatively the same as that for $HB(OH)_2$, the same conclusion should be applicable for reactions of real boranes experimentally studied. It involves oxidative addition the B−H bond of borane to the catalyst, followed by coordination of olefin to the complex between B and H ligands. The reaction further proceeds by insertion of C=C into the Rh−B bond, followed by the coupling of H and C_2H_5BR or dehydrogenative reductive elimination of C_2H_5BR to give the product complex and eventual dissociation of the C_2H_5BR. The activation energy for the last two steps of the mechanism, reductive elimination and dissociation, is calculated to be about 20 kcal/mol. Since in solution the endothermicity for the dissociation would be reduced by solvating of the regenerated catalyst, the coupling of H and C_2H_5BR is the rate-determining step. Our conclusion agrees with experimental observation of the reductive elimination step is the slowest in overall transformation.[2-4]

The other competitive mechanism (**II.2**) begins with addition of olefin to the catalyst. The next step is σ-bond metathesis, i.e., coordination of borane to the complex accompanied by simultaneous cleavage of Rh−C and B−H bonds with formation of B−C and Rh−H bonds. After an internal rotation, which does not require high activation energy, dehydrogenative reductive elimination of C_2H_5BR take place. The final steps for mechanism **II.2** coincide with those for mechanism **I.1.B**, and the rate-determining barrier for **II.2** corresponding to the metathesis process, 23.9 kcal/mol, is not much higher than that barrier for **I.1.B**, 22.4 kcal/mol. However, along the **II.2** pathway, the system has to overcome both of these barriers.

Mechanisms **I.2** and **I.3**, merging with **II** at **a22**, have the same rate-controlling step as **II.2**, because reductive elimination of borane from **a16** and **a19** requires lower energy lost, 17.6 and 13.7 kcal/mol, respectively, than the activation energy for the σ-bond metathesis, 23.9 kcal/mol. Hence, mechanism **I.2** and **I.3** are also competitive with **II.2** and **I.1.B**.

If the system has a choice for C−C bond insertion into Rh−B or B−H with formation of a C−B bond, or to insert into Rh−H or B−H with formation of a C−H bond, the former process is always significantly more advantageous kinetically. Therefore, mechanisms **I.1.A** and **II.1** for the reaction of catalytic hydroboration seem to require high temperatures.

Potential energy surfaces for two reactions considered here appear to be very similar with the potential energy surface calculated for the reaction of catalytic hydroboration of C_2H_4 by BH_3, $RhCl(PH_3)_2 + C_2H_4 + BH_3 \rightarrow RhCl(PH_3)_2 + C_2H_5BH_2$.[19] It means that presence of oxygen atoms in borane does not directly affect the reaction mechanisms studied here. We of course find that O atoms stabilize some intermediate complexes, like **a12′** and **a14′**, by formation of Rh−O chelate bonds, but their effects on the overall potential energy profile are not evident. We require more studies to understand why Rh(I)-catalyzed olefin hydroboration has been observed only with boranes that contain B−O bonds.

In the present paper, we have not considered some aspects of Rh(I)-catalyzed olefin hydroboration, worthwhile to be studied in future. For instance, another reaction mechanism, involving dissociation of one of the phosphine ligands of the catalyst after oxidative addition of borane and coordination of olefin, is possible, as shown at the top of Scheme 1. Neither have we compared hydroboration reaction of terminal alkenes and highly substituted olefins, although the reaction rate is sensitive to the substitution pattern.[2-4] Theoretical calculations on these questions are now under way.

Acknowledgment. The authors are grateful to Profs. T. B. Marder and A. H. Hoveyda for stimulating discussions. This work was in part supported by the National Science Foundation.